ISBN: 978-3-95450-132-8 doi:10.18429/JACoW-IPAC2014-WEPRO022

MODAL ANALYSIS OF HELICAL UNDULATOR RADIATION IN CYLINDRICAL WAVEGUIDE*

T. Vardanyan#, M. Ivanyan, V. Sahakyan, A. Tsakanian, G. Zanyan,
CANDLE SRI, Yerevan, Armenia

Abstract

The helical undulators are widely used for the generation of the circular polarized electromagnetic radiation. Most works on the helical undulator refer to radiation in free space. We studied the influence of cylindrical waveguide with ideal conducting walls on the undulator radiation of the relativistic point charge moving with helical orbit along the waveguide axes. The radiation field configurations are derived using the modal expansion technique. The comparison with free space results was made for radiation power.

INTRODUCTION

The helical undulators play an important role as the source of circular polarized electromagnetic radiation for wide range of research fields based on spin resolved photoelectron spectroscopy, the circular dichroism and etc. [1]. The spectral range of this radiation may vary from THz to X-ray regions. In a real device the spectral, polarization and spatial characteristics of undulator radiation are modified by the boundary conditions of the surrounding vacuum chamber [2, 3]. Considering the vacuum chamber as a cylindrical waveguide the radiated fields are modified by the waveguide boundary conditions and the radiated energy is redistributed among waveguide modes. As a result, the continuous energy spectrum transforms into discrete spectrum lines with sharp peaks, each corresponding to an exited waveguide mode. The knowledge about the peculiarities of radiation redistribution in a real device is important both from the radiation, FEL physics and the beam dynamics point of view .

In this report, the relativistic charge radiation in helical undulator with surrounding cylindrical waveguide of circular cross section and perfect conducting walls is studied. The radiated energy discrete spectrum is calculated and compared with the free space radiation. The energy distribution in TM and TE modes of the waveguide are determined. The numerical results for the planed THz coherent radiation source at the AREAL test facility [4] are presented.

FIELD CONFIGURATIONS

Consider the point charge q moving along a helical orbit inside a cylindrical waveguide with circular cross section of radius b and the ideal conducting walls. The charge ρ and current densities $\vec{j}$ for such a motion in cylindrical coordinates (r, φ, z) are given as

$$\rho = q\frac{\delta(r-a)}{r}\delta(\varphi-\omega_0 t)\delta(z-Vt) \qquad (1)$$

$$\vec{j} = (\omega_0 a\vec{e}_\varphi + V\vec{e}_z)\rho \qquad (2)$$

where ω_0 is the particle revolution frequency, v - the particle longitudinal velocity, a - the helix radius, $\vec{e}_\varphi, \vec{e}_z$ - the corresponding unit vectors. The periodic magnetic field $\vec{B}$ on the axis of the helical undulator is given by

$$\vec{B} = B_0[\vec{e}_r\, cos(kz-\varphi) + \vec{e}_\varphi\, sin(kz-\varphi)] \qquad (3)$$

with $k = 2\pi/\lambda_u$, λ_u - the helical winding period along the undulator axis. An important feature of the particle motion in purely helical undulator is that the longitudinal velocity is a constant, given by

$$v = c\left(1-\frac{1+K^2}{2\gamma^2}\right) \qquad (4)$$

where K is the dimensionless undulator deflection parameter, γ is the particle Lorenz factor.

As the undulator radiation is in forward direction and concentrated within a central cone with an opening angle of γ^{-1}, for the long small gap undulators the presence of the chamber walls modifies the scattered radiated fields forming the set of the propagating modes in the waveguide. In addition, the radiation spectrum transforms into discrete spectrum.

The radiated fields in the waveguide are defined by the Maxwell's equations with the boundary conditions of vanishing the tangential component of the electric field at the waveguide walls, i.e. $E_z = E_\varphi = 0$ at $r = b$.

With the use of the modal expansion technique [5] it can be shown that the radiated fields in the waveguide are composed of both types of propagating modes: TM and TE modes. The longitudinal components of electric (TM modes) and magnetic (TE modes) fields are expressed as following:

TM Modes

$$E_z = \sum_{n,m=1}^{\infty} Q_{nm} J_n(\alpha_{nm}\, r/b)\cdot e^{i(n\varphi+zf_{nm}-t\omega_{nm})} \qquad (5)$$

with

*This work was supported by State Committee of Science MES RA, in frame of the research project № SCS 13YR-1C0056
#tvardanyan@asls.candle.am

Content from this work may be used under the terms of the CC BY 3.0 licence (© 2014). Any distribution of this work must maintain attribution to the author(s), title of the work, publisher, and DOI.

ISBN: 978-3-95450-132-8 doi:10.18429/JACoW-IPAC2014-WEPRO022

$$\omega_{nm} = \frac{D_{nm}\beta_z + n\omega_0}{(1-\beta_z^2)}, \quad f_{nm} = \frac{n\omega_0\beta_z + D}{c(1-\beta_z^2)} \tag{6a}$$

$$Q_{nm} = \frac{q}{2\pi\varepsilon b^2}\frac{J_n(\alpha_{nm}a/b)}{J'^2_n(\alpha_{nm})} \tag{6b}$$

$$D_{nm} = \sqrt{n^2\omega_0^2 - (1-\beta_z^2)x_{nm}^2}, \quad x_{nm} = \alpha_{nm}c/b \tag{6c}$$

TE modes

$$H_z = \sum_{n,m=1}^{\infty} K_{nm}J_n(\alpha'_{nm}r/b)e^{i(n\varphi+zh_{nm}-tg_{nm})} \tag{7}$$

with

$$K_{nm} = \frac{iqc\omega_0 a}{2\pi b^2}\frac{\alpha'^2_{nm}}{\alpha'^2_{nm}-n^2}\frac{J'_n(\alpha'_{nm}a/b)}{J_n^2(\alpha'_{nm})G_{nm}}, \tag{8a}$$

$$h_{nm} = \frac{n\omega_0\beta_z + G}{c(1-\beta_z^2)}, \quad g_{nm} = \frac{G_{nm}\beta_z + n\omega_0}{(1-\beta_z^2)} \tag{8b}$$

$$G_{nm} = \sqrt{n^2\omega_0^2 - (1-\beta_z^2)y_{nm}^2}, \quad y_{nm} = \alpha'_{nm}c/b \tag{8c}$$

In (5)-(8) α_{nm} and α'_{nm} are the zeros of the first order Bessel functions J_n and its derivative J'_n respectively ($J_n(\alpha_{nm}) = 0, J'_n(\alpha'_{nm}) = 0$) $\beta_z = v/c$.

From expression under root in (6) and (8) it is easy to obtain the condition for non-vanishing modes.

$$n\omega_0 > x_{nm}\sqrt{1-\beta_z^2} \qquad n\omega_0 > y_{nm}\sqrt{1-\beta_z^2}$$

As we are interested only in propagating waves, we neglect the $n=0$ mode in (5), (7). The field transverse components are derived from the Maxwell equations.

RADIATED ENERGY ALONG WAVEGUIDE

The energy flow for monochromatic waves is described by the complex Poynting vector

$$\vec{S} = \frac{1}{2}\left[\vec{E}\times\vec{H}\right] \tag{9}$$

the real part of which gives the time-averaged energy flow. The transverse component of $\vec{S}$ represents reactive energy flow and does not contribute to the time-averaged flux of energy. The axial component of Poynting vector gives the time-averaged flow of energy along the guide. To evaluate the total power flow P we integrate the axial component of $\vec{S}$ over the cross-section of waveguide.

$$P_z = \frac{1}{2}\int_0^b\int_0^{2\pi}\left[\vec{E}\times\vec{H}^*\right]\cdot\vec{e}_z r dr d\varphi \tag{10}$$

Using field transverse components from appendix it is easy to get expression for power flow in waveguide TM_{nm} and TE_{nm} modes

$$P^{TM}_{z,nm} = -\frac{\pi\varepsilon b^4}{\alpha^4_{nm}}Q^2_{nm}f_{nm}\omega_{nm}\int_0^b F(\alpha_{nm},r)rdr \tag{11}$$

Radiated power flow along waveguide for TE mode

$$P^{TE}_{z,nm} = -\frac{\pi\mu b^4}{\alpha^4_{nm}}K^2_{nm}h_{nm}g_{nm}\int_0^b F(\alpha'_{nm},r)dr \tag{12}$$

where

$$F(x,r) = J'^2_n(xr/b) + \frac{n^2}{r^2}J_n^2(xr/b)$$

Numerical Example for AREAL

One of the outlooks of the 20 MeV AREAL RF photogun linac [4] which is under construction at CANDLE is the creation of THz coherent radiation station based on the helical undulator. In this section, the spectrum and the power of the point charge radiation are presented using the typical undulator parameters for THz radiation given in Table1. The particles energy and the bunch charge are 12.3MeV and 100pC respectively.

Table 1: Helical Undulator Parameter List

Period	8 cm
Number of periods	13
Peak field	0.1 T
Undulator constant K	0.75

Table 2 presents the predicted radiation characteristics for the 12.3 MeV energy electron beam for free space. The helix radius is 0.04 cm with the particle revolution frequency of 0.023 THz.

Table 2: Free Space Radiation Characteristics

Expected rad. Freq. in 1st harmonic	2.78 THz
Particle total energy loss [μJ]	124.4
Maximum deflection angle[rad]	0.31
Central cone opening angle [rad]	0.45

The discrete spectrums of radiation in 1m long undulator section with 1 cm radius of the waveguide are shown in Fig.1 and Fig.2.

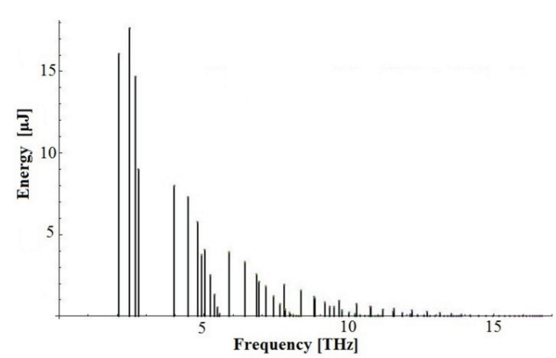

Figure 1: Discrete radiation energy spectrum of TM modes for waveguide radius equal to 1cm.

Content from this work may be used under the terms of the CC BY 3.0 licence (© 2014). Any distribution of this work must maintain attribution to the author(s), title of the work, publisher, and DOI.

ISBN: 978-3-95450-132-8 doi:10.18429/JACoW-IPAC2014-WEPRO022

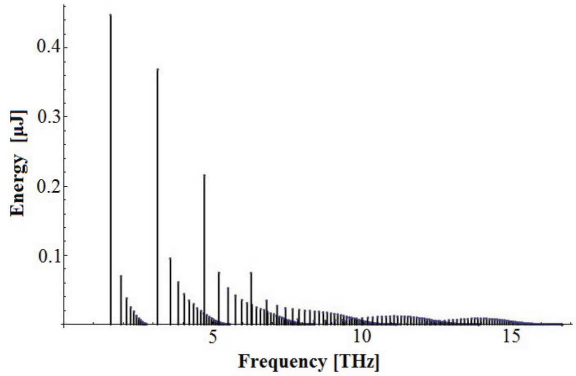

Figure 2: Discrete radiation energy spectrum of TE modes for waveguide radius equal to 1cm.

As it is seen, the total radiated energy is transformed into the TM and TE modes of the waveguide. The total radiated energy stored in TM modes is about 117μJ (~98%) for TM modes and 2.4μJ (~ 2%) for TE mode. The results are in good agreement with total radiated energy (124.4μJ) in free space from helical undulator.
In Fig 3 the shape of free space spectrum [6] is compared with TM and TE discrete spectrums given by (11) and (12). For the spectral intensity shape comparison, the line spectrum is multiplied by factor 10^{12}. The original line spectrum integration for total radiated energy gives 124.4μJ. As one can see, a good agreement of the radiation spectral shape is obtained.

The first radiation peak of the helical undulator in forward direction is reached at the resonant frequency

$$\omega_1 = \frac{2\pi c}{\lambda_u}\frac{2\gamma^2}{1+K^2} \qquad (13)$$

equal to 2.78 THz. For the waveguide undulator the narrow band spectrum is splitting into 4 discrete lines at frequencies 2.73, 2.62, 2.42 and 2.05 THz corresponding to the TM modes with indexes (11), (12), (13) and (14).

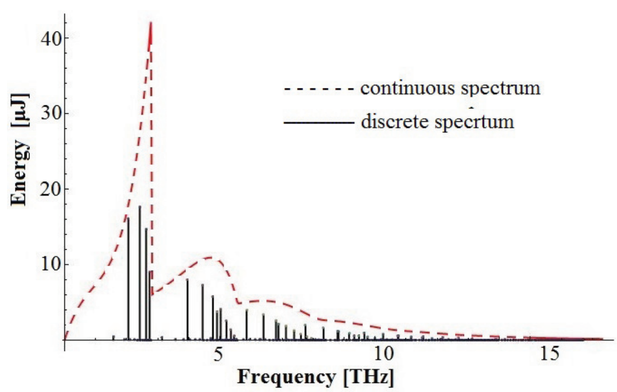

Figure 3: Comparison of the free space line spectrum shape with the waveguide undulator discrete spectrum.

For the larger waveguide radius the number of excited and propagating modes increases resulting to dense discrete lines in radiation spectrum. A smooth transition to free space radiation spectrum is observed. For smaller waveguide radius the number of propagating modes decreases. Although the total radiated energy is kept at the same level, the spectral distribution might differ from the free space radiation spectrum.

CONCLUSION

The influence of cylindrical waveguide for helical undulator radiation of charged particle was investigated. The expressions for the field components and radiated energy are obtained. The presence of waveguide leads to redistribution of continues spectrum to set of propagating waveguide modes. The numerical example for the THz helical radiation source for AREAL test facility is also discussed.

APPENDIX

The field transverse components for TE and TM modes

$$E_r^{TM} = -ib^2\sum_{n,m=1}^{\infty}\frac{f_{nm}}{\alpha_{nm}^2}Q_{nm}J'_n(\alpha_{nm}r/b)\times e^{i(n\varphi+zf_{nm}-t\omega_{nm})}$$

$$E_\varphi^{TM} = -\sum_{n,m=1}^{\infty}\frac{ib^2}{\alpha_{nm}^2}Q_{nm}f_{nm}\frac{in}{r}J_n(\alpha_{nm}r/b)\times e^{i(n\varphi+zf_{nm}-t\omega_{nm})}$$

$$H_\varphi^{TM} = i\varepsilon b^2\sum_{n,m=1}^{\infty}\frac{\omega_{nm}}{\alpha_{nm}^2}Q_{nm}J'_n(\alpha_{nm}r/b)\times e^{i(n\varphi+zf_{nm}-t\omega_{nm})}$$

$$H_r^{TM} = -i\varepsilon b^2\sum_{n,m=1}^{\infty}\frac{\omega_{nm}}{\alpha_{nm}^2}Q_{nm}\frac{in}{r}J_n(\alpha_{nm}r/b)\times e^{i(n\varphi+zf_{nm}-t\omega_{nm})}$$

$$E_r^{TE} = \mu b^2\sum_{n,m=1}^{\infty}\frac{g_{nm}}{\alpha_{nm}'^2}K_{nm}\frac{n}{r}J_n(\alpha'_{nm}r/b)e^{i(n\varphi+zh_{nm}-tg_{nm})}$$

$$E_\varphi^{TE} = i\mu b^2\sum_{n,m=1}^{\infty}\frac{g_{nm}}{\alpha_{nm}^2}K_{nm}J'_n(\alpha'_{nm}r/b)e^{i(n\varphi+zh_{nm}-tg_{nm})}$$

$$H_\varphi^{TE} = -b^2\sum_{n,m=1}^{\infty}\frac{h_{nm}}{\alpha_{nm}^2}K_{nm}\frac{n}{r}J_n(\alpha'_{nm}r/b)e^{i(n\varphi+zh_{nm}-tg_{nm})}$$

$$H_r^{TE} = ib^2\sum_{n,m=1}^{\infty}\frac{h_{nm}}{\alpha_{nm}^2}K_{nm}J'_n(\alpha'_{nm}r/b)e^{i(n\varphi+zh_{nm}-tg_{nm})}$$

REFERENCES

[1] H. Onuki and P. Ellaume, Wigglers, Undulators and Their Applications, New-York, Taylor & Francis, 438 p. 2004.
[2] G. Geloni et al., Proceedings of FEL2007, Novosibirsk, Russia, MOPPH009, 34, 37.
[3] S. K. Chhotray, G. Mishra, Physics Letters A 268, 1-11, (2000) .
[4] B. Grigoryan, et al., Proceedings of IPAC2011, San Sebastian, Spain, TUPC031, 1066, 1068.
[5] R. E. Collin, "Field Theory of Guided Waves", McGrew-Hill, New York, 1960.
[6] B. M. Kincaid, J. Of App. Phys., Vol. 48 p. 2684 (1977).

Content from this work may be used under the terms of the CC BY 3.0 licence (© 2014). Any distribution of this work must maintain attribution to the author(s), title of the work, publisher, and DOI.